# Chapter 1
# A Pipeline for Automated Coordinate Assignment in Anatomically Accurate Biventricular Models

Lisa Pankewitz[1], Laryssa Abdala[2], Aadarsh Bussooa[1], Hermenegild Arevalo[1]

1 – Simula Research Laboratory, Norway
2 – University of North Carolina, USA

**Abstract** There is an increased interest, in the field of cardiac modeling, for an improved coordinate system that can consistently describe local position within a heart geometry across various distinct geometries. A newly designed coordinate system, Cobiveco, meets these requirements. However, it assumes the use of biventricular models with a flat base, ignoring important cardiac structures. Therefore, we extended the scope of this state-of-the-art biventricular coordinate system to work with various heart geometries which include basal cardiac structures that were previously unaccounted for in Cobiveco. First, we implemented a semi-automated input surface assignment for increased accessibility and reproducibility of assigned coordinates. Then, we extended the coordinate system to handle more anatomically accurate biventricular models including the valve planes, which are of great interest when modeling diseases that manifest themselves in the basal area. Furthermore, we added the functionality of mapping vector data, such as myocardial fiber orientations, which are crucial for replicating the anisotropic electrical propagation in cardiac tissue.

## 1.1 Introduction

The representation of cardiac geometry independent of patient origin and the flawless transfer between different measuring modalities are important tools in clinical research [1, 2]. To accurately describe a local position within the heart, a robust coordinate system is required. Such a coordinate system enables a variety of applications, including the transfer of data between different heart geometries and comparing data produced using different measuring modalities, such as validating simulations with clinical data [2, 3].



K. J. McCabe (ed.), *Computational Physiology*, Simula SpringerBriefs on Computing 12, https://doi.org/10.1007/978-3-031-05164-7_1

A recently published biventricular coordinate system, Cobiveco, offers a consistent and reliable approach for describing positions in biventricular heart models [2]. However, the current state-of-the-art coordinate system is limited to biventricular heart geometries, which are clipped at a specific planar position, such that the resulting base appears completely flat. Clipping the base in this manner also clips the underlying ventricles. Although this clipping procedure remains part of the common mesh generation approach, it does not yield anatomically accurate cardiac meshes for the purpose of computer simulations. We argue that biophysical simulations of the heart should include the clipped base cardiac structures, that contain the valve openings, for more realistic results. The ventricles, together with the presence of valve planes, are important features of ventricular anatomy that can influence cardiac electrophysiology and mechanics.

Features that are connected to the valves are critical anatomical structures, such as the papillary muscle and chordae. Any structural defects that change the shape of the ventricles and alter the activation in the aortic valve annulus can have an effect on electrical dyssynchrony or ventricular dilation. Therefore, the inclusion of valve planes in cardiac models is necessary. This is especially true when modeling certain disease phenotypes, where changes in anatomy, mechanics, and activation manifest themselves in areas closer to the valve planes. An important example of this is congenital heart defect (CHD), which is the most common birth defect worldwide [4, 5]. Heterogeneous morphology and physiology in CHD patients have been shown to complicate risk assessment of individual patients requiring anatomically accurate models. This is a use-case where the inclusion of valve planes in the biventricular models may lead to enormous improvement of the model quality as morphological changes as well as scar tissues in this patient group can be located close to the base.

## 1.2 Methods

In this work, we extend the open-source MATLAB implementation of Cobiveco for tetrahedral meshes to take into account anatomically more accurate biventricular meshes that include valve planes instead of a flat, clipped base. First, we provide a surface extraction tool that automatically creates input surfaces files required for setting up the biventricular coordinate system. Then, we adapt the existing Cobiveco framework to allow for more anatomically correct geometries. Last, we extend the software to allow for mapping and transfer of vector data between different heart geometries.

### 1.2.1 Semi-Automated Surface Extraction

Existing tools extract surfaces from meshes and imaging data. Image-based surface extraction operates directly on raw clinical imaging to identify cardiac structures,

effectively building a mesh with automated tagging of surfaces. Mesh-based surface extraction operates directly on the meshes and identifies cardiac structures based on the position and connectivity of vertices. However, these currently existing tools require much fine-tuning and cannot effortlessly extract surfaces based solely on a seed point and a threshold.

Therefore, we present a mesh-based surface extraction tool, which identifies cardiac structures using a minimal set of parameters. As a first step, the cardiac mesh is converted into a graph, where its nodes encode vertex identifiers and surface identifiers. We leverage the use of the graph topology and apply a breadth-first search (BFS) algorithm to find connected nodes.

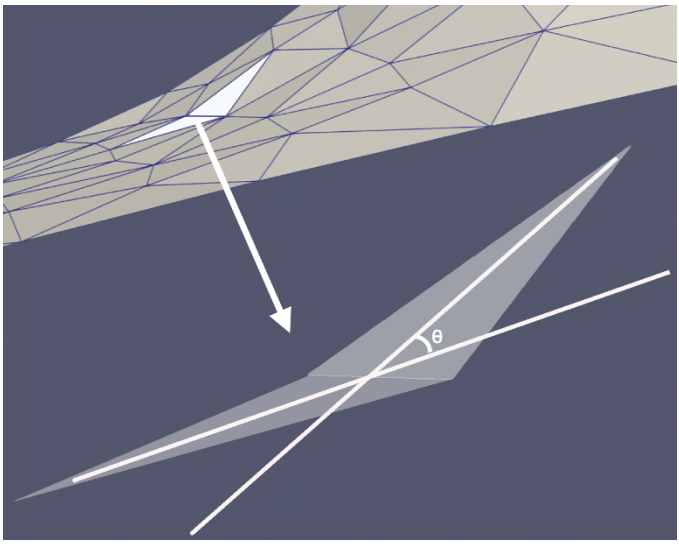


Fig. 1.1: Angular change between two neighbouring triangular surfaces, given by $\theta$.

The scope of the BFS algorithm is limited by two parameters, namely a seed point lying on the surface to be extracted and an angular threshold. The BFS algorithm performs several iterations, starting with the seed point. With each iteration, the angular change between two neighbouring triangles is computed, such that they comply with the stated threshold.

$$\cos\theta = \frac{n_1 \cdot n_2}{|n_1||n_2|} \tag{1.1}$$

The angular change is given in (1.1), where $n_1$ and $n_2$ are the normals to two triangular surfaces (Figure 1.1). These two triangles do not have to be direct neighbours to each other. The BFS algorithm identifies neighbours in the vicinity, using a predefined depth variable, such that the overall algorithm achieves a faster execution time. The pseudo code of the implementation is given in Algorithm 1.

**Algorithm 1** Algorithm to identify connected mesh nodes

```
tagged ← seed                                   ▷ Source seed point is added to tagged list
for tag in tagged do
    results ← bfs_tree(source=tag)              ▷ Apply BFS algorithm to tagged surfaces
    for res in results do
        angular_change = compute_angle(tag, res)   ▷ Angular change between tag and res
        if angular_change < angular_threshold then
            tagged ← res                        ▷ Add the res point to the tagged list
        end if
    end for
end for
```

The algorithm mimics edge detection, as used in image processing, where in our case the BFS spans throughout the mesh until sharp corners are encountered. Based on heuristics, we have identified that an angular threshold between 0.1 and 0.2 rad is optimal in correctly identifying and extracting cardiac structures in the mesh. In the context of extending the features of Cobiveco, the algorithm can be used to extract the base of the valves and the valve plane on the epicardial surface. The extracted base is excluded from the graph and subsequent surface extraction freely applies the BFS algorithm without any angular threshold restrictions.

### 1.2.2 Biventricular Coordinate System

Cobiveco, a **co**nsistent **bive**ntricular **co**ordinate system, provides a reliable framework for the precise and intuitive description of the position in the heart. To consistently describe a location within the heart, the coordinate system is established with four coordinates. The coordinate system fulfils a set of desired properties, which have been described in Section 1.1. The system is based on a set of four coordinates, namely a transventricular coordinate (tr), a transmural coordinate (tm), a rotational coordinate (rt) and an apicobasal coordinate (ab). The transventricular coordinate is a binary coordinate which distinguishes between the left and right ventricle. The transmural coordinate measures the distance traveled within the transmural space, so in the free walls this refers to the distance from the epicardium to the endocardium. The rotational coordinate gives information about where you are in the heart with respect to anterior and posterior direction. In more detail, it refers to the distance traveled from the interventricular posterior junction over the the interventricular anterior junction over the septum back to the interventricular posterior junction. The rotational coordinate is set up symmetrical in the biventricular model. The apicobasal coordinate describes the distance traveled from the apex point to the base. Each coordinate tuple, consisting of the four coordinates, corresponds to exactly one point in the heart. Coordinates are normalized and range between 0 and 1. Within that range, all coordinates change linearly in space, indicating that the distance traveled is directly proportional to the change in the coordinate of interest. Furthermore, both

ventricles follow the same parametrization. This is also reflected in the shared apex definition. To construct the coordinate system, only landmarks which are consistent throughout variations in different geometries, are chosen.

#### 1.2.2.1 Creation of the Coordinate System Cobiveco

A detailed description of the steps involved in the creation of the original Cobiveco framework can be found in [2]. In short, the construction of the coordinate system includes eight steps and is summarized below.

As with Cobiveco 1.0, Cobiveco 2.0 requires a biventricular volume that includes a base containing the four heart valve annuli, including the connecting bridges. Besides the volume mesh, five boundary surfaces as shown in Figure 1.3 are required as input, which is one additional surface compared to Cobiveco 1.0. The surfaces required are a *basal surface* $S_{Base}$, a *basal epicardial surface* $S_{Epi,base}$, an *epicardial, non basal surface* $S_{Epi,\ nonbase}$, an *LV endocardial surface* $S_{LV}$ and an *RV endocardial surface* $S_{RV}$. The utilities for the semi-automated input-file generation are described in Section 1.2.1.

##### Transventricular Coordinate (tv)

The transventricular coordinate is calculated as described in the original publication [2].

##### Extraction of Septal Surface and Curve

The *septal surface* $S_{Sept}$ and the *septal curve* $C_{Sept}$ are extracted as described in [2].

##### Transmural Coordinate (tm)

The calculation of the transmural coordinate follows the same steps as in Cobiveco 1.0, but takes into account the two epicardial surfaces. As we split the epicardial surface into a non-base epicardial surface and a basal epicardial surface, the whole epicardial surface is defined be the union of both, as given in (1.2):

$$S_{\text{Epi}} = S_{\text{Epi\_non\_base}} \cup S_{\text{Epi\_base}} \tag{1.2}$$

##### Heart Axes and Apex Point

The definition of the heart axes and apex point mainly follows the steps described in the original publication [2]. As the definition of the orthogonal heart axes largely

depends on the truncated septal surface, the calculation of the truncation needed to be revised to take into consideration the increased curvature of the septal surface at the base of the anatomically accurate biventricular heart model. Therefore the septal surface is additionally truncated by 15% at the basal side, where the distance is based in the direction of $\mathbf{v}_{\mathbf{LongAx}}$. This modification results in the final truncated septal surface $S_{SeptTrunc}$ being calculated by (1.3), where $\mathrm{P}_q$ refers to the $q^{th}$ percentile.

$$S_{\mathrm{SeptTrunc}} = \{\mathbf{x} \in S_{\mathrm{Sept}} \mid \mathbf{x} \cdot \mathbf{v}_{\mathrm{AP}} > \mathrm{P}_{20}(\mathbf{x} \cdot \mathbf{v}_{\mathrm{AP}}) \text{ and } \mathbf{x} \cdot \mathbf{v}_{\mathrm{AP}} < \mathrm{P}_{90}(\mathbf{x} \cdot \mathbf{v}_{\mathrm{AP}})\} \text{ and } \mathbf{x} \cdot \mathbf{v}_{\mathrm{long}} > \mathrm{P}_{15}(\mathbf{x} \cdot \mathbf{v}_{\mathrm{long}})\} \tag{1.3}$$

Since the *septal curve* needs to be split in two segments, the new geometry with a closed base requires a different solution than in Cobiveco 1.0 as well. Hence, we exclude the new, *basal epicardial surface* from the epicardial definition to allow for a separation of the anterior and posterior part of the septal curve.

$$C_{\mathrm{Sept}} = \{\mathbf{x} \in S_{\mathrm{Epi,base}} \mid u_v(\mathbf{x}) = 0.5\} \tag{1.4}$$

### Extraction of Ridge Surfaces

As the more anatomically accurate biventricular models contain a closed surface at the base, we needed to modify the ridge definition in Cobiveco 2.0. In Cobiveco 2.0 we aim to replicate the original ridge assignment but use the valve planes as guiding points resulting in a symmetric ridge. The ridge is used to provide a boundary condition for the rotational coordinate. Currently, the ridge is defined from the posterior interventricular junctions, where both ventricles symmetrically impose a boundary condition, via the mitral valve and tricuspid valve in the LV/RV septum respectively. The anterior ridge definition is defined via the mitral valve and pulmonary valve, resulting in the ridge definition as shown in Figure 1.2.

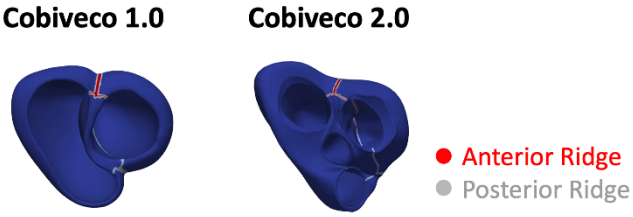


Fig. 1.2: Ridge definition in Cobiveco 1.0 and Cobiveco 2.0. The anterior part of the ridge is colored in red, while the posterior part of the ridge is highlighted in grey.

Therefore, the ridge is obtained by defining the solution to Laplace's equation with boundaries applied to be 0 on the epicardial basal surface and 1 on the septal surface. The *non-base epicardial surface* is now excluded as a boundary condition, as shown in (1.5).

$$\Delta u_{\text{Ridge}}(V) = 0 \quad \text{with} \quad u_{\text{Ridge}}\left(S_{\text{Epi}} \setminus S_{\text{Sept}}\right) = 0 \quad \text{and} \quad u_{\text{Ridge}}\left(S|_{\text{Sept}}\right) = 1 \tag{1.5}$$

The solution to Laplace's equation is calculated as shown here in (1.6).

$$\Delta u_{\text{Ridge}}(V) = 0 \quad \text{with} \quad u_{\text{Ridge}}\left(S_{\text{Epi,nonbase}} \setminus S_{\text{Sept}}\right) = 0 \quad \text{and} \quad u_{\text{Ridge}}\left(S|_{\text{Sept}}\right) = 1 \tag{1.6}$$

The second step remains as set up in the original Cobiveco 1.0. However, the resulting ridge cannot be applied as it is. Currently, a manual filtering step is involved as there remains a ridge within the RV in-between the tricuspid and the pulmonary valve, which is not used as a boundary condition when setting up the rotational coordinate.

#### The Rotational Coordinate (r)

The rotational coordinate is defined as described in [2].

#### Computation of the Apicobasal Coordinate (ab)

The apicobasal coordinate is calculated as described in the original Cobiveco article. Currently, however, we used the solution to Laplace's equation as a place holder, as the rotational coordinate still includes discontinuities which prohibit the assignment of the apicobasal coordinate as described in Cobiveco 1.0

### 1.2.3 Mapping Vector Fields

The original Cobiveco implementation has a scalar field mapping functionality available. To map a scalar field from the source mesh $B$ to a target mesh $A$, it constructs a matrix $M_{A \leftarrow B}$ from the nodes of the source mesh to the nodes of the target mesh [2]. The user can choose between linear and nearest-neighbor interpolation.

Mapping vector fields is of interest since data, such as muscle fiber fields, are crucial to advance the cardiovascular computational simulations field. Here we enable the functionality of mapping such fields by treating each coordinate as a scalar field. More specifically, the vector field is represented as a matrix of the nodes of the source mesh by three. Each of its columns represents the coordinate of the vector field in each source node. The end result of the vector mapping process is shown in Figure 1.5.

## 1.3 Results

In this project, we have successfully founded the basis for extending Cobiveco to include more anatomically accurate biventricular models. The results are presented in three steps, namely a pre-processing, processing, and post-processing step. Each step reduces the manual manipulation of meshes, generalizes the biventricular coordinates, and enables vector data transfer, respectively.

First, we successfully implemented a semi-automated surface extraction method that uses a minimal set of parameters, based on a seed point and angular threshold, to identify structures of interest in cardiac meshes. The resulting surfaces, after extraction, are shown in Figure 1.3.

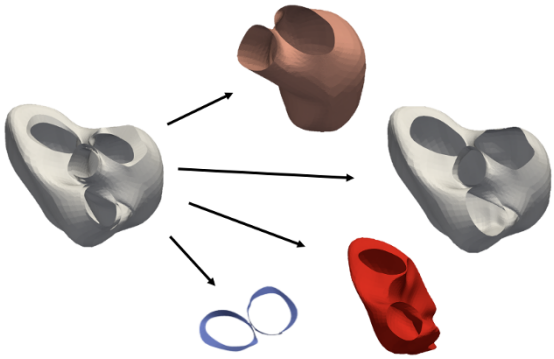

Fig. 1.3: Extracted surfaces after using BFS algorithm and angular threshold.

Second, we adapted the previous Cobiveco framework to work with biventricular geometries, which includes the four cardiac valve planes. The preliminary results of Cobiveco 2.0 are shown in Figure 1.4. The rotational coordinate suffers from inconsistencies at the septum, owing to the manual exclusion of the ridge boundary. Currently, the apicobasal coordinate is only represented by the solution to Laplace's equation. Last, we adapted the framework to include the mapping of vector data. The result for mapping synthetic data is shown in Figure 1.5.

## 1.4 Conclusion

In this project, we present an updated version of the consistent biventricular coordinates introduced by [2]. The pipeline can be applied to biventricular geometries for mapping scalar and vector data between different hearts.

Cobiveco 2.0 builds upon the original Cobiveco [2], by extending the coordinates for biventricular geometries that include the ventricular base. We aim to keep the

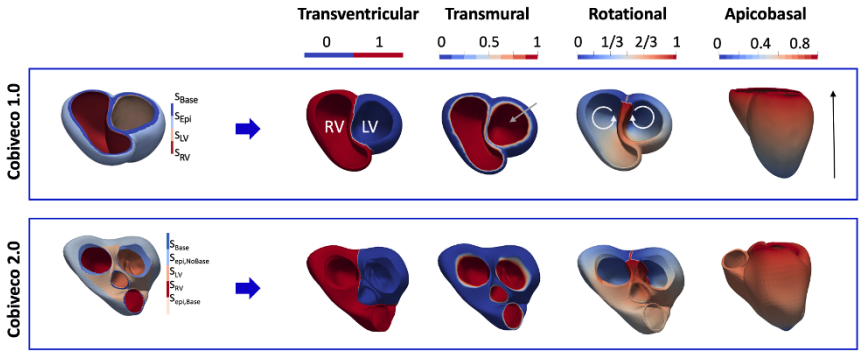


Fig. 1.4: Visual Comparison of the four coordinates created by Cobiveco 2.0 and Cobiveco 1.0. The apicobasal coordinate shown for Cobiveco 2.0 is represented by the solution to Laplace's equation.

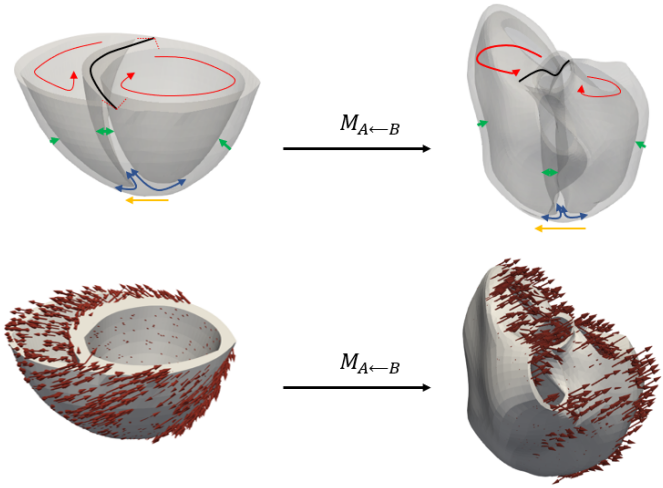


Fig. 1.5: Cobiveco 2.0 has the functionality of mapping vector fields. First, the coordinates are built in the source $B$ and target $A$ biventricular geometries (top). Then the map $M_{A \leftarrow B}$ is used to map vector fields (bottom).

resulting coordinates with the same properties from the original ones: bijective, continuous (apart from the binary transventricular coordinates), normalized, complete, linear, with consistent parametrization, and consistent landmarks.

The new pipeline reduces manual mesh manipulations for surface extraction. The required surfaces can be effortlessly extracted using fewer parameters than other conventional methods. Cobiveco 2.0 enables the mapping of vector data in addition to scalar data, which is useful for computational modeling and data comparison. A remarkable application of this feature is myofiber data mapping which is widely used in electrophysiology simulations. Moreover, by enabling data transfer between anatomical accurate biventricular geometries, it will be possible to validate computational models for diseases that manifest themselves in areas close to the valve planes.

The newly developed pipeline, with the inclusion of the valve planes in the cardiac model, is of special interest for studying the most common form of CHD, namely Tetralogy of Fallot (ToF). In ToF patients, the scar tissue is located close to the base, rendering electrophysiological simulations feasible with our pipeline [6, 7, 8, 9, 10, 11].

To the best of our knowledge, there is no consistent coordinate system available that can be readily applied to a four-chamber heart model. The current state-of-the-art coordinates for the atria, Universal Atrial Coordinates (UAC) is not based on circular coordinates but rather in lateral-septal and posterior-anterior coordinates [12]. The two-dimensional framework can be extended to three dimensions by adding a transmural coordinate. Therefore, merging our improved Cobiveco pipeline with an updated version of the UAC could be used to create a consistent four-chamber heart coordinate system.

### 1.4.1 Limitations

The limitations of the current work include incomplete assignment of the rotational and apicobasal coordinates. Therefore, we aim to improve the ridge assignment to obtain a more symmetric ridge, which will result in a more symmetric rotational coordinate, as the ridge defines the boundaries set in the rotational coordinate. To achieve this goal, we will modify the anterior part of the ridge in the LV to be defined via the aortic valve and not via the mitral valve as the definition is set now. This will ensure a symmetric set up of the rotational coordinate in the RV and LV. The remaining parts of the proposed framework, however, were successfully tested in one patient-specific geometry.

Besides, a statistical analysis of the errors using a cohort of geometries is necessary to ensure this is a reliable coordinate system. Moreover, the mappings were performed using artificial data. Future work could include transferring experimental data between two geometries to ensure the results are physiologically consistent. Furthermore, the post-processing could also feature tensor data mapping.

## References


1. Matthijs Cluitmans, Dana H Brooks, Rob MacLeod, Olaf Dössel, María S Guillem, Peter M van Dam, Jana Svehlikova, Bin He, John Sapp, Linwei Wang, et al. Validation and opportunities of electrocardiographic imaging: from technical achievements to clinical applications. *Frontiers in physiology*, 9:1305, 2018.
2. Steffen Schuler, Nicolas Pilia, Danila Potyagaylo, and Axel Loewe. Cobiveco: Consistent biventricular coordinates for precise and intuitive description of position in the heart–with matlab implementation. *arXiv preprint arXiv:2102.02898*, 2021.
3. Jason Bayer, Anton J Prassl, Ali Pashaei, Juan F Gomez, Antonio Frontera, Aurel Neic, Gernot Plank, and Edward J Vigmond. Universal ventricular coordinates: A generic framework for describing position within the heart and transferring data. *Medical Image Analysis*, 45:83–93, 2018.
4. Bryan Boling. *Cardiothoracic Surgical Critical Care, An Issue of Critical Care Nursing Clinics of North America, E-Book*, volume 31. Elsevier Health Sciences, 2019.
5. Christian Apitz, Gary D Webb, and Andrew N Redington. Tetralogy of fallot. *The Lancet*, 374(9699):1462–1471, 2009.
6. R Bedair and X Iriart. Educational series in congenital heart disease: Tetralogy of fallot: diagnosis to long-term follow-up. *Echo Research and Practice*, 6(1):R9–R23, 2019.
7. Sara Piran, Anne S Bassett, Jasmine Grewal, Jodi-Ann Swaby, Chantal Morel, Erwin N Oechslin, Andrew N Redington, Peter P Liu, and Candice K Silversides. Patterns of cardiac and extracardiac anomalies in adults with tetralogy of fallot. *American heart journal*, 161(1):131–137, 2011.
8. Sotiria C Apostolopoulou, Athanassios Manginas, Nikolaos L Kelekis, and Michel Noutsias. Cardiovascular imaging approach in pre and postoperative tetralogy of fallot. *BMC cardiovascular disorders*, 19(1):1–12, 2019.
9. Ariane J Marelli, Andrew S Mackie, Raluca Ionescu-Ittu, Elham Rahme, and Louise Pilote. Congenital heart disease in the general population: changing prevalence and age distribution. *Circulation*, 115(2):163–172, 2007.
10. Wei Hui, Cameron Slorach, Andreea Dragulescu, Luc Mertens, Bart Bijnens, and Mark K Friedberg. Mechanisms of right ventricular electromechanical dyssynchrony and mechanical inefficiency in children after repair of tetralogy of fallot. *Circulation: Cardiovascular Imaging*, 7(4):610–618, 2014.
11. Charlotte Brouwer, Gijsbert FL Kapel, Monique RM Jongbloed, Martin J Schalij, Marta de Riva Silva, and Katja Zeppenfeld. Noninvasive identification of ventricular tachycardia–related anatomical isthmuses in repaired tetralogy of fallot: What is the role of the 12-lead ventricular tachycardia electrocardiogram. *JACC: Clinical Electrophysiology*, 4(10):1308–1318, 2018.
12. Caroline H Roney, Ali Pashaei, Marianna Meo, Rémi Dubois, Patrick M Boyle, Natalia A Trayanova, Hubert Cochet, Steven A Niederer, and Edward J Vigmond. Universal atrial coordinates applied to visualisation, registration and construction of patient specific meshes. *Medical image analysis*, 55:65–75, 2019.